

AD-A259 728



WL-TR-91-4102



HIGH RESOLUTION COMPUTED TOMOGRAPHY

Richard H. Bossi
John L. Cline
Gary E. Georgeson

Boeing Aerospace & Electronics
P.O. Box 3999
Seattle, WA 98124

July 1992

Interim Report for Period August 1990 - May 1991

Approved for public release; distribution is unlimited

DTIC
ELECTE
JAN 27 1993
S C D

MATERIALS DIRECTORATE
WRIGHT LABORATORY
AIR FORCE SYSTEMS COMMAND
WRIGHT-PATTERSON AIR FORCE BASE, OHIO 45433-6533

93-01454




3908


NOTICE

When Government drawings, specifications, or other data are used for any purpose other than in connection with a definitely Government-related procurement, the United States Government incurs no responsibility or any obligation whatsoever. The fact that the government may have formulated or in any way supplied the said drawings, specifications, or other data, is not to be regarded by implication, or otherwise in any manner construed, as licensing the holder, or any other person or corporation: or as conveying any rights or permission to manufacture, use, or sell any patented invention that may in any way be related thereto.


This report is releasable to the National Technical Information Service (NTIS). At NTIS, it will be available to the general public, including foreign nations.

This technical report has been reviewed and is approved for publication.


CHARLES F. BUYNAK
Nondestructive Evaluation Branch
Metals and Ceramics Division


TOBEY M. CORDELL, Chief
Nondestructive Evaluation Branch
Metals and Ceramics Division

FOR THE COMMANDER


DR. NORMAN M. TALLAN, Director
Metals and Ceramics Division
Materials Directorate

If your address has changed, if you wish to be removed from our mailing list, or if the addressee is no longer employed by your organization please notify WL/MLLP, WPAFB, OH 45433-6533 to help us maintain a current mailing list.

Copies of this report should not be returned unless return is required by security considerations, contractual obligations, or notice on a specific document.

REPORT DOCUMENTATION PAGE			Form Approved OMB No. 0704-0188	
1. AGENCY USE ONLY (Leave Blank)	2. REPORT DATE July 31, 1992	3. REPORT TYPE AND DATES COVERED Interim Aug. 1990 - May 1991		
4. TITLE AND SUBTITLE High Resolution Computed Tomography		5. FUNDING NUMBERS F33615-88-C-5404 PE: 63112F PR: 3153 TA: 00 WU: 06		
6. AUTHOR(S) Richard H. Bossi, John L. Cline and Gary E. Georgeson				
7. PERFORMING ORGANIZATION NAME(S) AND ADDRESS(ES) Boeing Defense & Space Group P.O. Box 3999 Seattle, WA 98124-2499		8. PERFORMING ORGANIZATION REPORT NUMBER		
9. SPONSORING/MONITORING AGENCY NAME(S) AND ADDRESS(ES) Charles Buynak (513) 255-9802 Wright Laboratory, Materials Directorate (WL/MLLP) Wright-Patterson AFB, OH 54533-6533		10. SPONSORING/MONITORING AGENCY REPORT NUMBER WL-TR-91-4102		
11. SUPPLEMENTARY NOTES				
12a. DISTRIBUTION/AVAILABILITY STATEMENT Approved for public release; Distribution is unlimited		12b. DISTRIBUTION CODE		
13. ABSTRACT (Maximum 200 words) High resolution (greater than 4 line pairs per millimeter) computed tomography (CT) has been studied for its potential use for engineering evaluation of aerospace components. The CT images provide two dimensional maps of material linear x-ray attenuation coefficients for small volume elements, smaller than 0.001 cubic millimeters. These images are similar to micrographic images of polished surfaces from sectioned components, but are achieved nondestructively. For investigating materials where destructive sectioning relieves stresses, changing the internal configuration of features, such as gaps, high resolution CT provides superior diagnostic information for engineering evaluation. The primary benefits of CT are realized in accelerating schedules through faster data acquisition and reducing engineering risk by providing increased information nondestructively. High resolution CT is particularly well suited to assist in failure analysis investigations. Multiple slice or volume reconstruction high resolution CT can provide full three dimensional models. The cost and performance of high resolution CT systems are functions of the component size and ultimate resolution capability. For many common evaluation needs, the capital cost can be as low as a 50 percent cost add-on to a real-time radiographic imaging system. Relative to micrography, CT can be performed in about one-fifth the time, depending on the number of samples.				
14. SUBJECT TERMS High Resolution, Microfocus, Characterization, X-Ray, Micrography, Computed Tomography (CT), Failure Analysis, Nondestructive Evaluation (NDE)		15. NUMBER OF PAGES 38 16. PRICE CODE		
17. SECURITY CLASSIFICATION OF REPORT Unclassified	18. SECURITY CLASSIFICATION OF THIS PAGE Unclassified	19. SECURITY CLASSIFICATION OF ABSTRACT Unclassified	20. LIMITATION OF ABSTRACT UL	

TABLE OF CONTENTS

Section	Page
1.0 INTRODUCTION	1
1.1 Computed Tomography	1
1.2 Scope and Objective	2
2.0 TEST PLAN	3
2.1 Part Acquisition	3
2.2 CT Testing	3
2.3 Data Evaluation	5
3.0 RESULTS	6
3.1 Noninvasive Micrography	6
3.1.1 Material Characterization	6
3.1.2 Structural Characteristics	10
3.2 Failure Analysis	15
3.2.1 Manufacturing Flaws	15
3.2.2 Damage Measurement	17
4.0 COST BENEFIT ANALYSIS	24
4.1 Noninvasive Micrography	24
4.2 Failure Analysis	26
5.0 CONCLUSIONS AND RECOMMENDATIONS	27
5.1 Conclusions	27
5.2 Recommendations	27
6.0 REFERENCES	28
APPENDIX A	31
APPENDIX B	32

DTIC QUALITY INSPECTED 5

Accession For	
NTIS CHAM	<input checked="" type="checkbox"/>
DTIC TAB	<input type="checkbox"/>
Unannounced	<input type="checkbox"/>
Justification	
By	
Distribution/	
Availability Codes	
Avail and/or	
Dist	Special
A-1	

LIST OF FIGURES

Figure		Page
3.1-1	Photograph of SiC coated carbon matrix composite.	7
3.1-2	Photomicrograph of the sectioned SiC coated carbon matrix composite surface (7 x 7 mm).	7
3.1-3	CT slice of the SiC sample, contrast set for coating evaluation from System W.	8
3.1-4	Same CT slice as Figure 3.1-3 with the contrast set for the core evaluation.	8
3.1-5	CT slice of the SiC sample, contrast set for coating evaluation from System X.	9
3.1-6	Same CT slice as Figure 3.1-5 with the contrast set for the core evaluation.	9
3.1-7	Photograph of a potted, sectioned rivet.	11
3.1-8	CT slice through the rivet test sample.	11
3.1-9	Photograph of the sectioned rivet test sample.	11
3.1-10	CT slice of the sample after sectioning.	11
3.1-11	Photograph of a portion of a ceramic filter.	12
3.1-12	Photomicrograph of the sectioned ceramic filter (5 x 5 mm).	12
3.1-13	CT slice of the ceramic filter.	13
3.1-14	CT slice of the ceramic filter showing 50 μ m pores.	13
3.1-15	CT images of four consecutive slices of the ceramic filter on System V.	14
3.2-1	Photograph of three fiber optic connectors.	15
3.2-2	A series of CT slices in an optic connector showing bond voids and off-centering of the fiber.	16
3.2-3	Photograph of a graphite epoxy panel that has been impact tested.	17
3.2-4	Ultrasonic time-of-flight C scan image of the impact damaged, graphite epoxy panel.	17
3.2-5	CT image of the impact damaged, graphite epoxy panel.	18
3.2-6	Photograph of a 20 mm x 45 mm section removed from the impacted panel.	18
3.2-7	High resolution CT images of the impacted graphite epoxy composite sample. Top edge is the impacted surface. Image locations are: a) center, b) 5 mm off center and c) 10 mm off center.	19
3.2-8	CT image of impact coupon for System V, 65 minute scan.	20
3.2-9	CT image of impact coupon from System V, 1 minute scan.	20
3.2-10	CT image of impact coupon from System X, 5 minute scan.	20
3.2-11	3D rendering of the impacted panel delaminations viewed at 0°.	21
3.2-12	Histogram of the delamination indications as a function of depth.	21
3.2-13	Eleven images of the delamination planes from the impacted panel.	22
3.2-14	3D rendering of the impacted panel delaminations viewed at 15°.	23
4.1-1	Cost benefits of CT for non-invasive micrography.	24
4.1-2	Comparison of the cost in hours of micrography and CT for the examination of one sample with multiple slices.	25

4.1-3	Comparison of the cost in hours of micrography and CT for the examination of multiple samples.	25
4.1-4	Comparison of the cost of slicing samples using CT or micrography as a function of the number of samples.	26

LIST OF TABLES

Table		Page
2.2-1	Potential High Resolution CT Systems	4
2.2-2	X-ray Intensity	4

ACKNOWLEDGEMENTS

Samples used for the example images were obtained from various Boeing organizations and companies involved in aerospace materials. Thanks are due to Mark Proulx and John Strupp of Boeing, and to Hi-Tech Ceramics. Special thanks are expressed to BIR, WL and Moltech for their generous effort in support of CT scanning.

SUMMARY

Under a preliminary testing task assignment of the Advanced Development of X-ray Computed Tomography Application program, high resolution (greater than 4 line pairs per millimeter) computed tomography (CT) has been studied for its potential use for engineering evaluation of aerospace components. High resolution CT images provide two dimensional maps of material linear X-ray attenuation coefficients for small volume elements, smaller than 0.001 cubic millimeters. These images are similar to micrographic images of polished surfaces from sectioned components, but are achieved nondestructively. For investigating materials where destructive sectioning relieves stresses, changing the internal configuration of features, such as gaps, high resolution CT provides superior diagnostic information for engineering evaluation.

The primary benefits of CT are realized in accelerating schedules through faster data acquisition and reducing engineering risk by providing increased information nondestructively. High resolution CT is particularly well suited to assist in failure analysis investigations. Multiple slice or volume reconstruction high resolution CT can provide full three dimensional models. The cost and performance of high resolution CT systems are functions of the component size and ultimate resolution capability. For many common evaluation needs the capital cost can be as low as a 50 percent cost add-on to a real-time radiographic imaging system. Relative to micrography, CT can be performed in about one-fifth the time, depending on the number of samples.

DISCLAIMER

The information contained in this document is neither an endorsement nor criticism for any X-ray imaging instrumentation or equipment used in this study.

1.0

INTRODUCTION

The goal of the Advanced Development of X-Ray Computed Tomography Applications demonstration (CTAD) program is to evaluate inspection applications for which X-ray computed tomography (CT) can provide a cost-effective means of evaluating aircraft/aerospace components. The program is "task assigned" so that specific CT applications or application areas can be addressed in separate projects. Three categories of task assignments are employed in the program: 1) preliminary tests where a variety of parts and components in an application area are studied for their suitability for CT examinations; 2) final tests, where one or a few components are selected for detailed testing of CT capability to detect and quantify defects; and 3) demonstrations, where the economic viability of CT for the evaluation of problems are analyzed and the results presented to government and industry. This interim report is the result of a preliminary task assignment study on the use of high resolution CT systems for aircraft/aerospace materials and components. Additional task assignment reports issued by the CTAD program are listed in references 1 through 10.

1.1

Computed Tomography

X-ray computed tomography (CT) is a powerful nondestructive evaluation technique that was conceived in the early 1960's and has been developing rapidly ever since. CT uses measurements of X-ray transmission from many angles about a component to compute the relative X-ray linear attenuation coefficient of small volume elements and presents them as a cross sectional image map. The clear images of an interior plane of an object are achieved without the confusion of superposition of features often found with conventional film radiography. CT can provide quantitative information about the density/constituents and dimensions of the features imaged.

Although CT has been predominantly applied to medical diagnosis, industrial applications have been growing over the past decade. Medical systems are designed for high throughput and low dosages specifically for humans and human sized objects. These systems can be applied to industrial objects that have low atomic number and are less than one-half meter in diameter. Industrial CT systems do not have dosage and size constraints. They are built in a wide range of sizes from the inspection of small jet engine turbine blades using mid-energy (hundreds of kV) X-ray sources to the inspection of large ICBM missiles requiring high (MV level) X-ray energies.

The resolution of CT systems is fundamentally determined by the beam width of the X-ray optics design, and is driven by the selection of source and detector aperture sizes and the source, object and detector distances. The beam width, size of the object and CT image reconstruction matrix must all be considered in a system design. At the present time the typical reconstruction matrix size for CT is 1024 x 1024. To a first approximation this would make the resolution limit roughly 1 part in 1000, and the system would be designed to match the X-ray optics to 1/1000th of the size of the part. For example a system designed to handle a 0.5 m size part might allow for 0.5 mm size beam width, and a system designed for a 10 mm size part might have a 0.010 mm beam width. It is of course possible, and routinely performed, to reconstruct the 1024 x 1024 matrix over subregions of a component so that a higher resolution beam width than 1 part in 1000 of the object can be used effectively. However, the scan must still cover the full size of the part. As the part size is increased, the source to detector distance increases, and the X-ray intensity at the detector falls off quadratically. Thus, it is impractical to use a very small beam width on large parts because of the very long scan time that will result. Practical resolutions for

CT systems that handle relatively large components (> 300 mm diameter) are in the range of 1 to 2 lp/mm. For components less than 300 mm diameter 2 to 4 lp/mm can be obtained. For higher resolution, greater than 4 lp/mm (feature sensitivity on the order of $125\text{ }\mu\text{m}$), CT systems are being designed that usually can handle parts of a few centimeters in size.

High resolution CT imaging has progressed along several lines of approach. By using fine collimation on CT systems capable of large (300 mm) fields of view it is possible to achieve high resolutions ($50\text{ }\mu\text{m}$ feature sensitivity) when a small field of view (50 mm) is used [11]. Specially designed detectors and a microfocus X-ray source have been used to achieve resolutions of better than $50\text{ }\mu\text{m}$ for material studies [12,13]. This capability is available as the Tomoscope[®] at the AF Wright Laboratories. Feldkamp [14] at Ford used a microfocus X-ray source and an X-ray image intensifier to develop a system capable of $20\text{ }\mu\text{m}$ resolutions in a volume reconstruction mode. An example of this capability was reported in an earlier CTAD task assignment report [4]. This approach is being developed by a number of research organizations including Argonne National Laboratory [15]. A commercially available product allows a microfocus X-ray source and image intensifier system to be converted into a high resolution CT system [16]. The volume approach to imaging for very high resolutions (down to $5\text{ }\mu\text{m}$) have been pursued by Lawrence Livermore National Laboratory [17] and Exxon [18]. Resolution down to a few micrometers is possible by combining high resolution detectors with synchrotron radiation sources [19,20,21,22]. Resolution in the few micrometer range is often referred to as X-ray microtomography.

1.2 Scope and Objective

This task assignment, designated "Task 10 - High Resolution CT," is a preliminary testing task directed at the evaluation of CT as an engineering evaluation tool for components that would benefit from cross sectional imaging at resolutions better than 4 lp/mm. The task assignment investigates the developments in high resolution CT systems and their potential benefit to the CTAD program goals.

A specific objective of this task assignment was to use higher resolution CT equipment on components from previous task assignments that were inadequately evaluated with CT systems with resolutions of 2 lp/mm and less. The higher resolution offers the capability of CT to provide noninvasive micrography information and this was investigated for its usefulness to the aircraft/aerospace industry.

2.0 TEST PLAN

The preliminary testing of high resolution CT involved the acquisition of test components, CT scanning on appropriate equipment, data evaluation, preliminary economic assessment, and reporting. Sensitivity to fine detail (on the order of 0.1 mm (0.004 inch) or smaller) is a problem with CT systems designed to handle components with sizes greater than 100 mm (4 inches). When a system can handle large parts, the data acquisition to provide very high resolution becomes impractical due to X-ray flux limitations for the X-ray beam width required. Therefore, for high resolution CT imaging, the component size must be scaled to the sensitivity required and the system optimized for that level of resolution performance.

2.1 Part Acquisition

Through the course of the CTAD program, a number of test articles have been obtained for which the evaluation required greater detail sensitivity than could be obtained on standard industrial CT systems available. Appendix A lists a number of components obtained, their part identification number (PID#), size and features of interest. Generally, the components are in need of a high resolution, nondestructive imaging technique that can view the interior material configuration.

2.2 CT Testing

CT testing at appropriate facilities was based on the availability of CT systems identified as potential high resolution CT imagers. Table 2.2-1 lists CT system types that have been identified as having high resolution capability. The high resolution CT capability fits into several categories: conventional, minifocus and microfocus X-ray sources with discrete detectors, linear detector arrays or image intensifiers. These systems may use fan beam or cone beam geometries. Of course variations to these general themes may be used in assembling a high resolution CT system.

Synchrotron source parallel beam/area array detector systems provide the highest resolution capability for CT imaging. However the part size must be small. This technology requires the availability of beam time at a synchrotron source. It is still considered to be a laboratory research tool for material studies and not presently practical of general aerospace industrial application. However, several significant future developments may change this such as the use of characteristic target energy X-ray tubes, small low cost industrial synchrotron sources and electron microscope based CT systems [17,23].

Table 2.2-1 Potential High Resolution CT Systems

(Values are order of magnitude estimates of system characteristics. Resolution is affected by the component size, such that the maximum resolution may not be achievable for the maximum allowable component size.)

System Type	Nominal Resolution	Approx. Max. Part Size	System Designator
Conventional X-Ray Source Fan Beam/Discrete Detectors	4 lp/mm	300 mm	B
Minifocus X-Ray Source Fan Beam/Discrete Detectors	10-20 lp/mm	50 mm	X
Microfocus X-Ray Source Fan Beam/Image Intensifier	10-20 lp/mm	100 mm	W
Microfocus Source Fan Beam/Linear Array Detector	10-20 lp/mm	100 mm	V
Microfocus Source Cone Beam/Image Intensifier	10-20 lp/mm	50 mm	
Synchrotron Source	20-40 lp/mm	5 mm	

The resolution of the CT system is determined by the X-ray optics design employed. Essentially the X-ray beam width in the part determines the inherent resolution of the system. The highest resolution capability would have an infinitely small X-ray beam, however such a beam would be require an infinitely large intensity for measurements to made. The trade-off between having a large intensity and a small beam size is driven by the capability of existing X-ray source technology. Scan time is a variable that can compensate for low intensity but still, scans must be reasonably fast (in the range of minutes) for a system to have practical applicability to industry.

A conventional approach to high resolution imaging is to use small detectors, or very tight collimation on the detectors, in a fan array and a small X-ray source. Small X-ray sources are readily available using microfocus technology which allows X-ray spot size in the range of 10 μm and smaller. The X-ray intensity from these sources is of course greatly reduced over regular X-ray sources. Table 2.2-2 lists the relative intensities of X-ray systems as a function of spot size, energy and maximum current allowed for some representative CT X-ray sources.

Table 2.2-2 X-ray Intensity

Spot Size (mm)	Energy (kV)	Current (mA)	Maximum Load (W)
0.01	160	0.06	10
0.05	160	0.6	100
0.2	160	1.9	300
0.4	160	4	640
1.2	320	3	960
0.8	420	2	840
1.5	420	5	2100

Reduction in the X-ray source size requires a reduction in the X-ray intensity available for imaging. For example, moving from a 1.2 mm, 320 kV, 3 mA source to a 0.01 mm, 160 kV, 0.06 mA source is approximately a factor of 200 drop in X-ray intensity, assuming the X-ray photon intensity is proportional to the square of the peak energy. To maintain similar data acquisition rates for scanning, the X-ray source-to-detector distance would need to be reduced by a factor of 14 ($[200]^{1/2}$). For high resolution imaging this is very practical. The spot size is reduced by a factor of over 120, yet the size of the object need only be reduced by a factor of 14. In fact, this effect allows considerable advantage for small object imaging, because projection magnification can be used. Although small, high resolution detectors can be constructed, they can be expensive and, depending upon the design are less efficient than large detectors. Using projection magnification allows a larger detector to be used, but still achieves the desired small X-ray beam width over the object.

High magnification (on the order of 10 or greater) normally results in limiting part sizes to less than 15 mm diameter using readily available technology. Balancing the part size, source size, detector aperture size and magnification are issues for high resolution CT system designers.

To overcome some of the source size limitations in conventional and microfocus X-ray sources, some researchers are using synchrotron radiation sources. The synchrotron provides a very high intensity parallel beam of monochromatic radiation achieved by the emission of photons from the curved trajectory of electrons that are circulating in a storage ring. Energies of 20 keV are typical with capability of up to 100 keV being possible. Tomography using synchrotron radiation can achieve resolution in the range of 1 to 5 μm . Sample sizes are of course small because at a resolution of 1 μm , a 1024 x 1024 image could only cover a 1 mm x 1 mm size sample. CT scanning on a synchrotron source can be expensive and must be performed based on the availability of a beam line at a suitable facility, of which there are only a few in the United States.

While high resolution CT systems of a number of different designs exist, the availability of these systems during the course of this task assignment was limited. This report shows representative CT imaging from only a few high resolution systems that are typical of the type that could be acquired for use in an industrial facility. In general the imaging quality of the high resolution CT systems is driven by the object size for which they are designed.

2.3 Data Evaluation

Data evaluation of the high resolution scans primarily consisted of comparison with destructive micrographic examination where possible. The images were evaluated for their ability to reveal information on interest and the usefulness of that information. Reproduction of the images in this report reduces the detail that can be observed in the original data viewed on an image display workstation.

3.0 RESULTS

High resolution CT imaging of components has resulted in the development of two major categories of application, noninvasive micrography and failure analysis. The components that have been tested have been categorized into these areas and the results of an example in each category presented. It is hoped that these examples will allow the readers to extrapolate to the benefits of high resolution CT imaging for their particular components.

Each component tested represents a particular problem having an objective, approach and payoff for using high resolution CT. Appendix B contains a summary of these issues for several examples that were tested.

3.1 Noninvasive Micrography

Noninvasive micrography refers to obtaining detailed information about the interior of an object without destructive sectioning. The CT images are maps of X-ray linear attenuation coefficient, which are different than optical reflection maps from cut surfaces. The CT images however are obtained without the damaging effects that will result when mechanical sectioning is performed. Mechanical sectioning damage can be surface distortions, release of residual stresses, insertion of new defects and destruction of valuable material. High resolution CT can be useful in micrographic studies when the materials have variations in X-ray linear attenuation coefficients such that the characteristics of interest can be identified. For example, features such as fibers, resins, voids, gaps, cracks, coatings and density variations can be identified.

3.1.1 Material Characterization

CT is effective for noninvasive micrography of material characteristics. For example, Figure 3.1-1 shows a photograph of a tensile specimen (PID# 0503015b) that is composed of a coating of SiC on a carbon matrix material. Micrography is used to evaluate the coating thickness and interface with the substrate (core) material of the specimen. Figure 3.1-2 is a photomicrograph of the sectioned surface taken after CT had been performed. Figures 3.1-3 and 3.1-4 are images from a CT slice of the sample taken on System W. The CT slice is taken through the center of the strain gauge measurement region. The contrast levels in Figures 3.1-3 and 3.1-4 are windowed to reveal details in the coating and the core respectively. Figures 3.1-5 and 3.1-6 are from a CT slice taken on a different high resolution CT system (System X) showing the coating and core material also. This CT slice is not at exactly the same location as the System W image. Both systems show good detail sensitivity to the coating thickness, coating migration into the structure and composite density variations.

The quality of the coating interface and the thickness are clearly indicated by CT. The resolution of features in these CT images are estimated at about 50 μm . The CT image (and the photomicrograph of the after test sectioned sample) shows that the strain gauge is mounted a significant distance from the actual material due to the mounting epoxy on a rough surface. This information can be used to evaluate the accuracy and validity of strain gauge results. The CT provides a volumetric measure of the distribution of material in the sample over the thickness of the CT slice. The photomicrographic results reveal information only on the surface based on optical reflection characteristics.

High resolution CT is useful for the evaluation of numerous types of material studies where sectioning is used to obtain important data. In the above case the data showed coating thickness and interface quality. CT can also show the material consistency and defects.

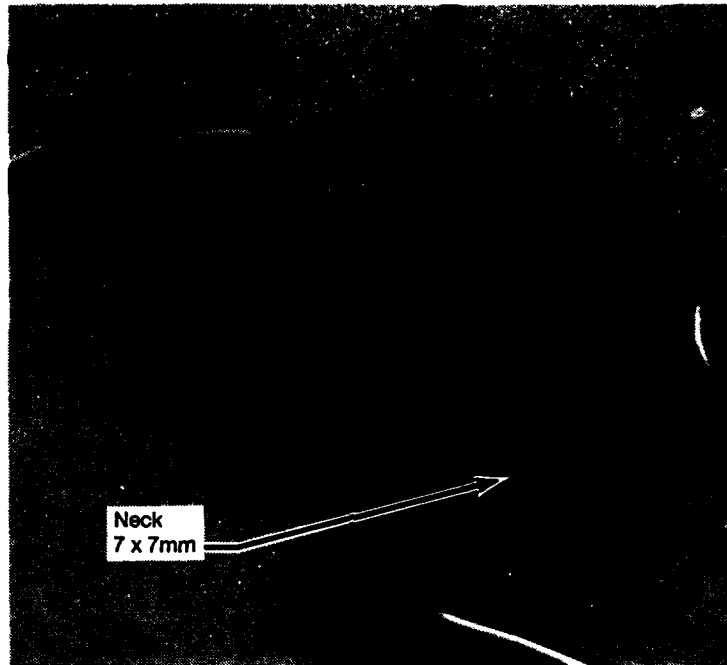


Figure 3.1-1 Photograph of SiC coated carbon matrix composite.



Figure 3.1-2 Photomicrograph of the sectioned SiC coated carbon matrix composite surface (7 x 7 mm) taken from the neck region of the Figure 3.1-1 tensile specimen.

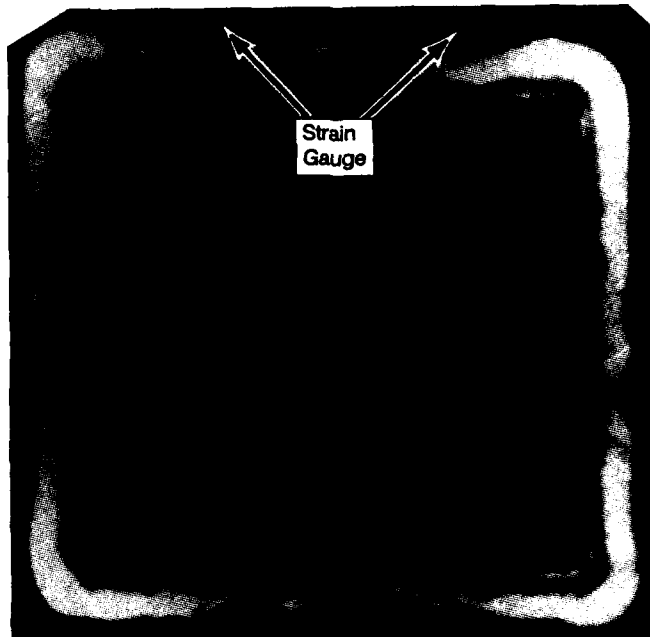


Figure 3.1-3 CT slice of the SiC sample, contrast set for coating evaluation from System W.

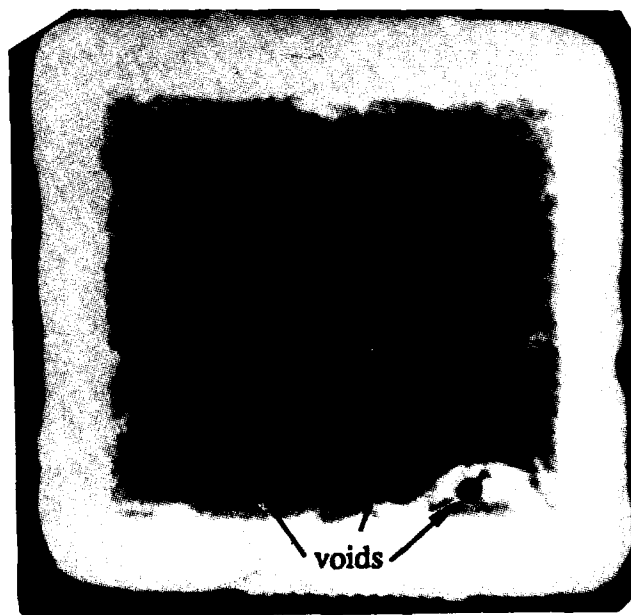


Figure 3.1-4 Same CT slice as Figure 3.1-3 with the contrast set for the core evaluation.



Figure 3.1-5 CT slice of the SiC sample, contrast set for coating **evaluation** from System X.



Figure 3.1-6 Same CT slice as Figure 3.1-5 with the contrast set for the **core** evaluation.

3.1.2 Structural Characteristics

Noninvasive micrography can play an even more important role in structure evaluation. Figure 3.1-7 shows a photograph of a squeeze riveting test sample (PID# 060311). The rivet fastens two 9.5 mm (3/8 inch) aluminum plates. In the past, potting and mechanical sectioning of test samples has been performed to evaluate the quality of the squeeze riveting process. Micrography is performed on the sectioned sample to measure gaps between the rivet and plates. In squeeze riveting, the intent is to fill the rivet hole. Oversqueezing will stress the hole while undersqueezing will leave a residual gap that can lead to fatigue cracking.

Computed tomography can be used as an alternative to sectioning. Figure 3.1-8 is a CT slice through the rivet sample before sectioning. The contrast in the image is enhanced, showing no gaps between the rivet and the holes in the aluminum plates, but enhancing the interface between the two plates. Figure 3.1-9 is a photograph of the rivet test sample after sectioning. Figure 3.1-10 shows a CT slice taken about 1 mm below the top surface. A gap is readily detected between the rivet and the holes in the plates. These results demonstrate importance of making measurements noninvasively. During sectioning, residual stresses are released and so the internal features, gaps in this case, are changed. The gaps in the sectioned rivet sample are measured to be about 50 μm maximum opening from both the CT data and from photographic measurements on the sectioned surface.

This result has significant consequences. First, the use of conventional micrography to study internal features that may be under stress is not practical because the features will move when the stress is altered by mechanical sectioning. CT sectioning is however noninvasive, showing the component and internal features as they actually exist. Second, the CT data can be analyzed in the before and after sectioning mode, to estimate the residual stress that was present because of the movement following sectioning, which relieved the stress. This calculation of course is no longer purely a noninvasive approach because it requires that the sample be sectioned to release the stress. Nevertheless, it is a new method that combines CT and micrography to obtain information about a structure that could not otherwise be obtained.

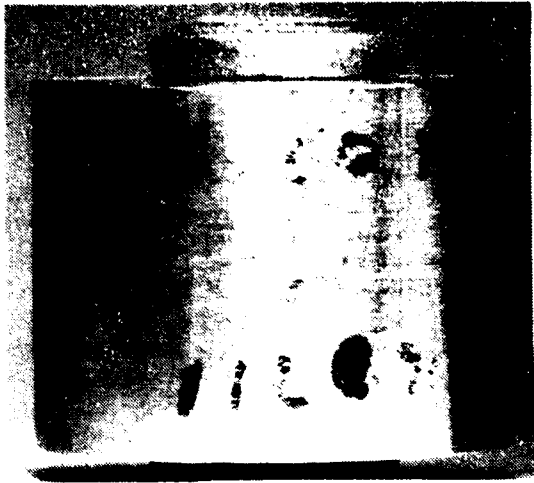


Figure 3.1-7 Photograph of a potted, sectioned rivet.

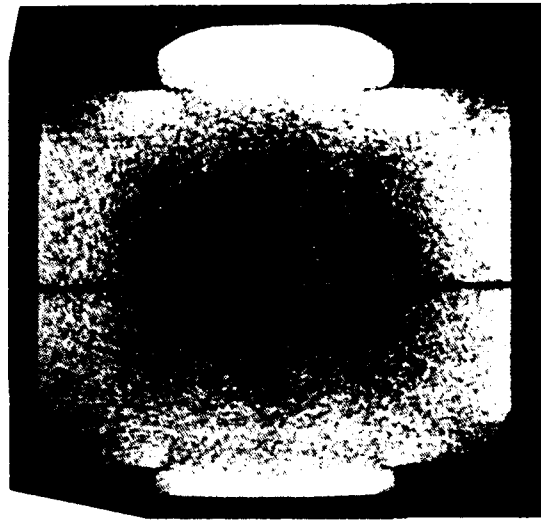


Figure 3.1-8 CT slice through the rivet test sample.

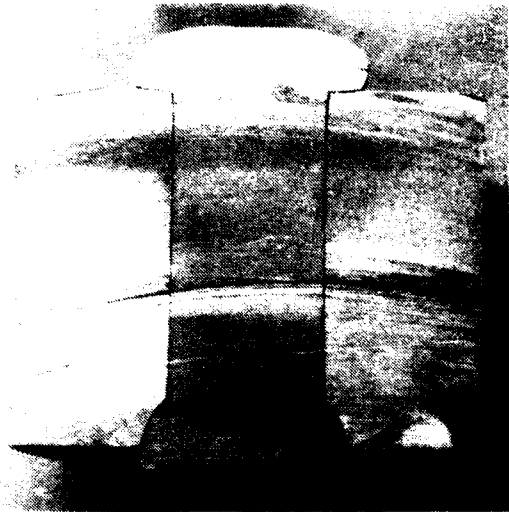


Figure 3.1-9 Photograph of the sectioned rivet test sample.

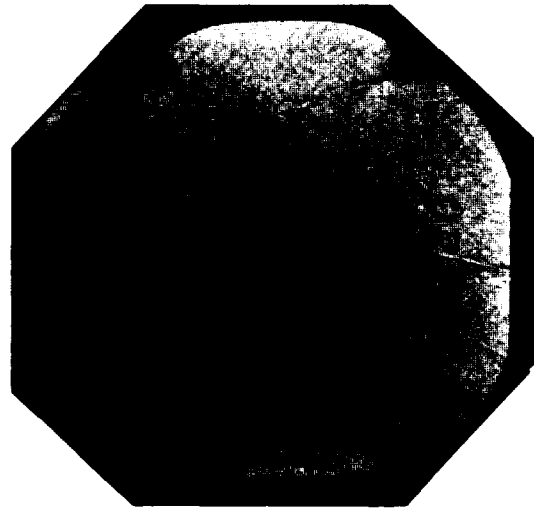


Figure 3.1-10 CT slice of the sample after sectioning.

Another example of studying a material structure is the case of porous ceramic filters that are used for filtering molten aluminum to produce high purity castings. The filter is manufactured with nominal holes ranging from 50 to 200 μm in diameter. Sectioning of a newly constructed filter is performed to determine not only pore size and shape, but a number of additional parameters which determine their ability to remove impurities [24]. Spent filters are sectioned to determine the type and distribution of contaminate material.

A photograph of a piece of a porous ceramic filter (PID# 050205) excised from a spent unit is shown in Figure 3.1-11. The ceramic filter matrix is almost hidden by the darker solidified aluminum. Figure 3.1-12 is a photomicrograph of a 5 x 5 mm square cross section of the ceramic filter piece. The aluminum is dark and the ceramic matrix is light. The surface was polished to 1 μm smoothness. Figures 3.1-13 and 3.1-14 are two representative CT slices taken across the excised filter section taken on System W. The CT image in Figure 3.1-13 compares approximately to the location for the photomicrograph, however the aluminum appears lighter in the CT image rather than darker as in the photomicrograph. This imaging capability shows the distribution of aluminum in the spent filter and residual pore openings, which are a small fraction in this sample. Figure 3.1-14 shows a portion of the filter that contains a region with little or no aluminum present. Pores of 50-60 μm in size are resolved and smaller pores are certainly detected. Figure 3.1-15 shows a series of four CT slices separated by 0.25 mm taken on System V. The images show a rapidly changing pattern in the direction of slice sequencing.

The CT data provides a method for evaluating the ceramic filter. Quantitative image analysis has recently been demonstrated on such images of ceramic filters to evaluate their structural quality, looking for void content, cell size and orientation [24,25].



Figure 3.1-11 Photograph of a portion of a ceramic filter.

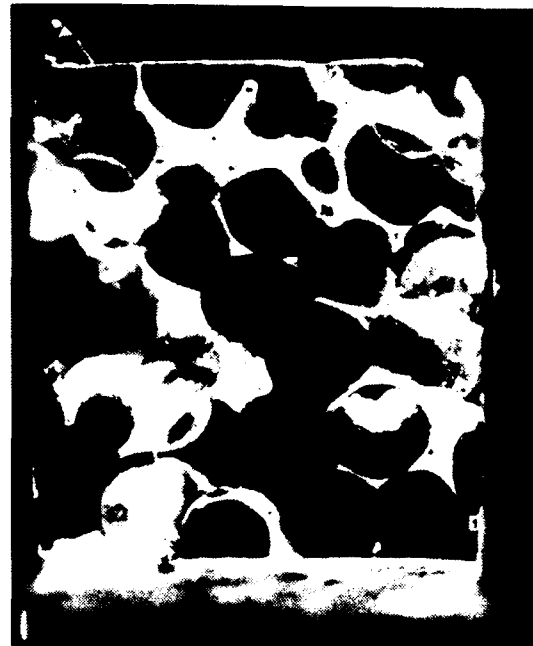


Figure 3.1-12 Photomicrograph of the sectioned ceramic filter (5 x 5 mm).

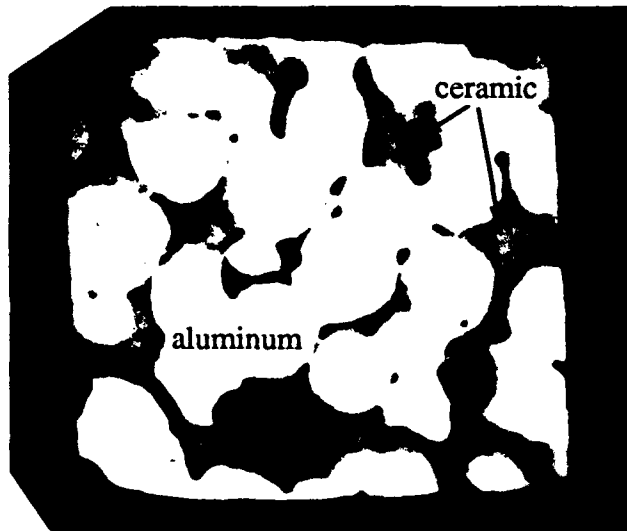


Figure 3.1-13 CT slice of the ceramic filter.

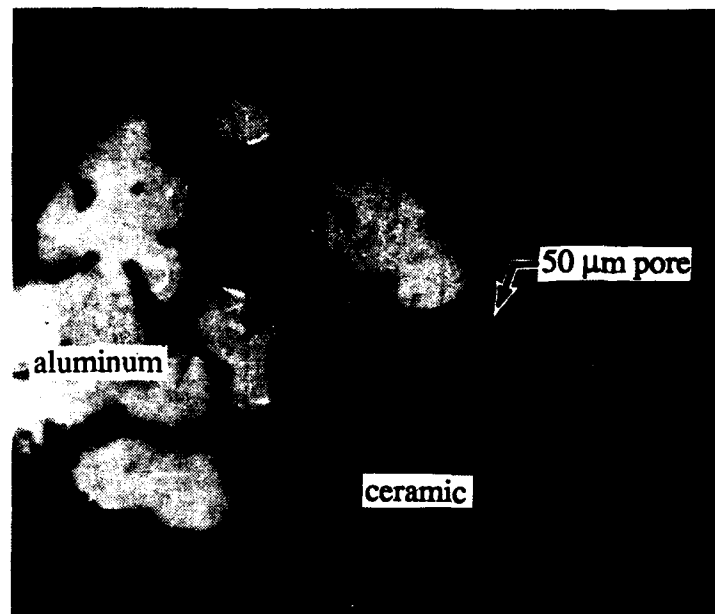


Figure 3.1-14 CT slice of the ceramic filter showing 50 μm pores.

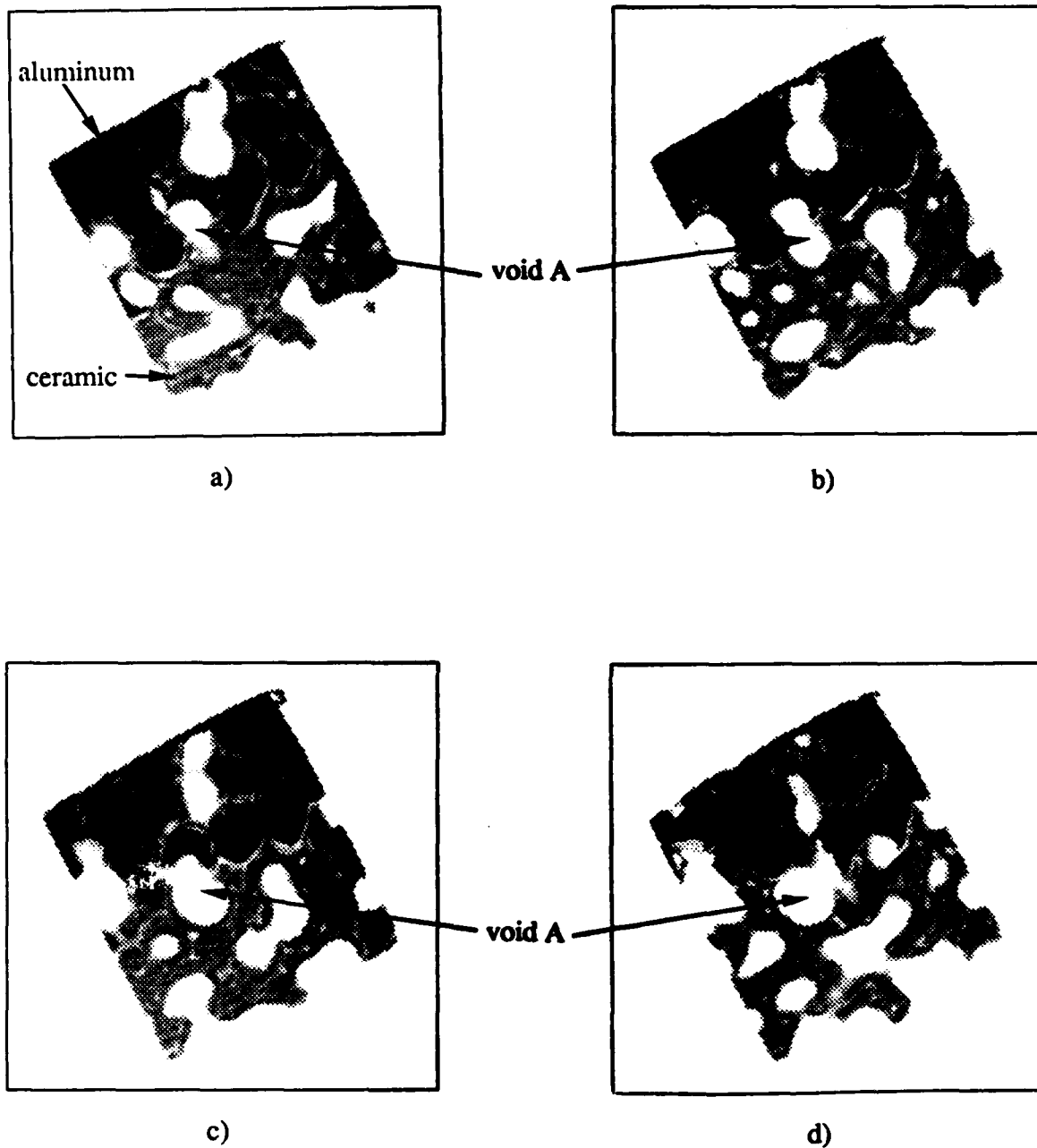


Figure 3.1-15 CT images of four consecutive slices of the ceramic filter on System V.

3.2 Failure Analysis

CT has been identified as a particularly good technique to be used in failure analysis studies. This has been identified in earlier CTAD reports [1,6] with the additional conclusion that microfocus real-time radiography can provide useful qualitative information in many cases. The high resolution capability of CT is effective when the features can not be separated in projection X-ray images, but require cross sectional views to determine the cause of failure.

3.2.1 Manufacturing Flaws

Often failure of a component is due to internal manufacturing features that are not adequately identified during the fabrication or which change due to use. Figure 3.2-1 is a photograph of three typical fiber optic connectors (PID# 010802). During the assembly of fiber optic connectors the central glass fiber is ideally oriented at the center of the protective fiber/sheath bundle. However it often migrates and may actually touch the side of the connector where it may sustain high signal loss or it may even be broken. Much of this damage is due to poor stripping of the cable prior to insertion into the connector and also poor bonding (voids) within the connector. There are currently no diagnostic tools for inspecting the concentricity or continuity of the central glass fiber or bond quality, once installed within the connector. A conductivity check is made on new cables and if there is a problem, the connector is scrapped. This happens often and is expensive.

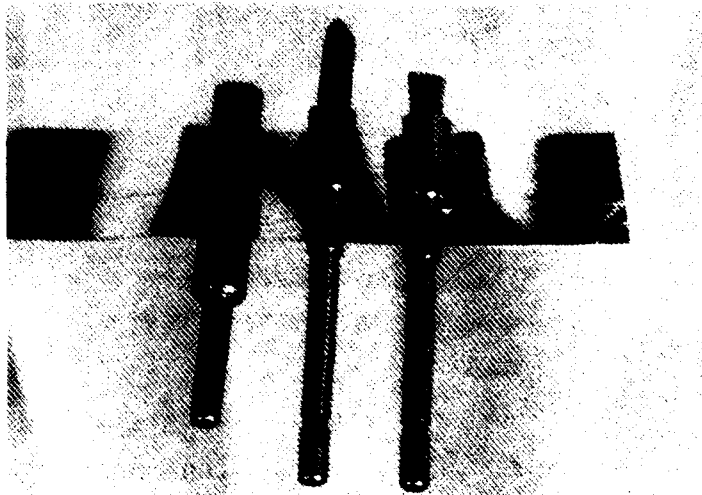


Figure 3.2-1 Photograph of three fiber optic connectors.

Figure 3.2-2 shows a series of CT slices across an optical connector and the relative slice location. The series identifies how the central fiber drifts off center. Scan numbers 3 and 4 in Figure 3.2-2 show severe (0.20 mm diameter) bonding voids (dark patches). Such information provides feedback information to the manufacturing process on the control of the fiber location and bond material.

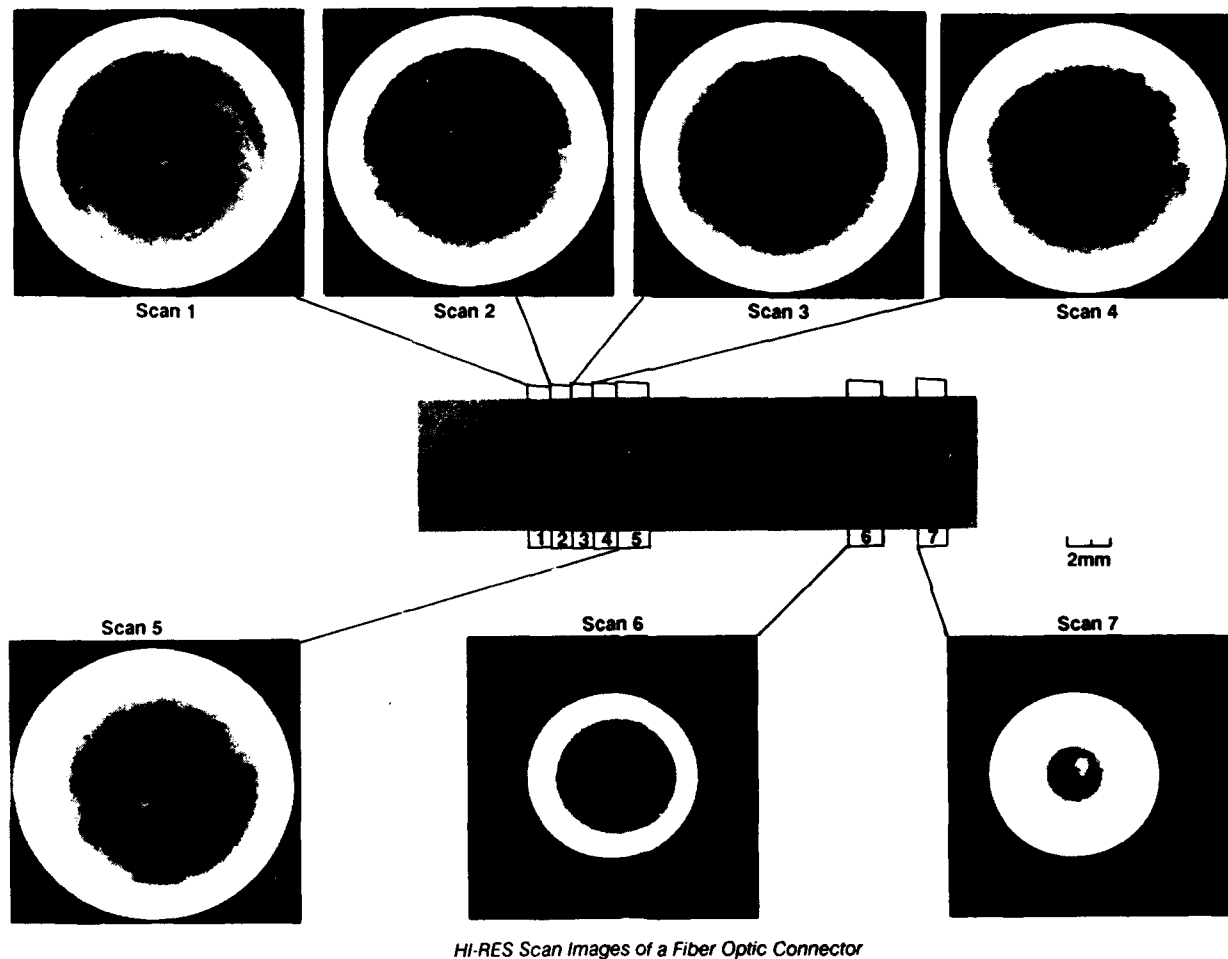


Figure 3.2-2 A series of CT slices in an optic connector showing bond voids and off-centering of the fiber.

3.2.2 Damage Measurement

The assessment of damage is an important part of failure analysis. One particular area of critical damage assessment is in organic composite laminates. When composite laminates are impacted the damage is manifested on multiple layers of the laminate. Ultrasonics is often used to evaluate the damage area and can show the pattern of damage as a function of the layer [26]. Figure 3.2-3 is a photograph of a 125 mm x 150 mm impact tested graphite epoxy test panel (PID# 040127). The laminate is 5 mm thick and was impacted with a 16 mm tup at 50 lbf. The impact damage area lies around the center and extends to about 20 mm in diameter. Figure 3.2-4 is the ultrasonic time-of-flight C-scan image showing the defect delamination pattern. Although the ultrasonic image shows the defect area, the delamination pattern on each layer is partially shadowed by the delamination of the layer above.

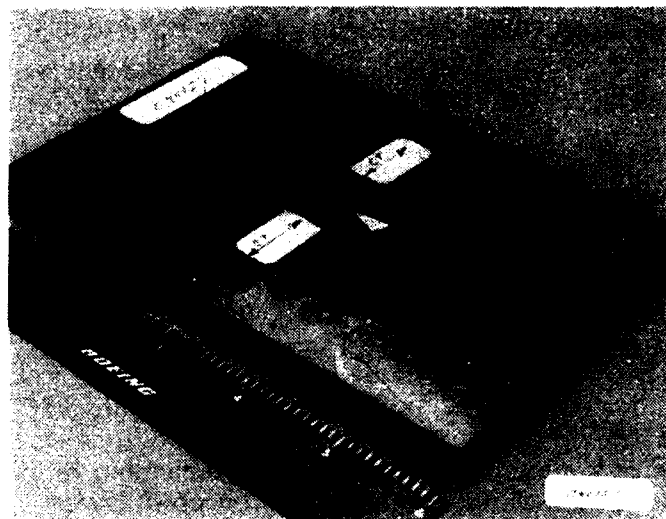


Figure 3.2-3 Photograph of a graphite epoxy panel that has been impact tested.

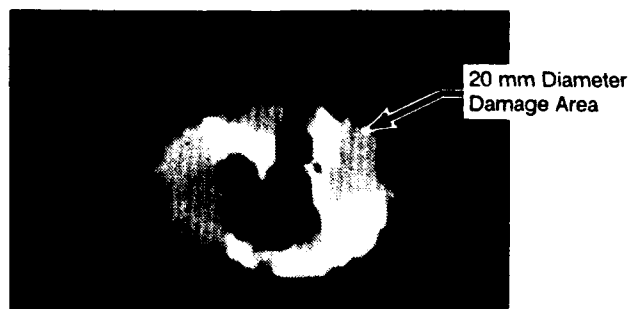


Figure 3.2-4 Ultrasonic time-of-flight C scan image of the impact damaged, graphite epoxy panel.

This impacted panel was scanned on a medium resolution CT system (2 lp/mm) and the CT image is shown in Figure 3.2-5. Some ply definition can be seen as well as a vague conical shaped damage pattern characteristic of impact damage in laminates.

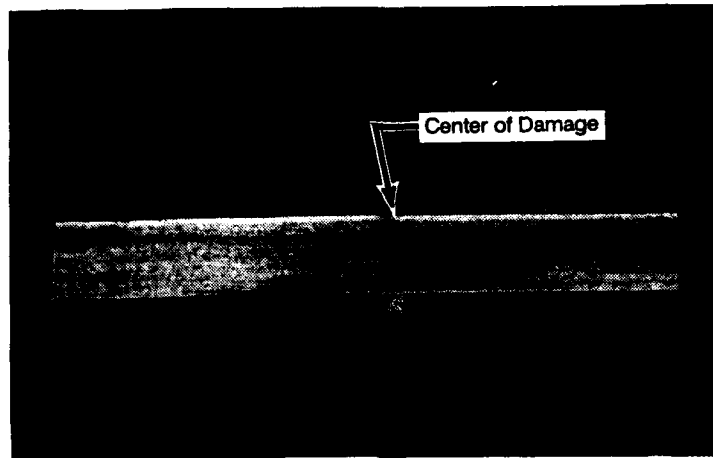


Figure 3.2-5 CT image of the impact damaged, graphite epoxy panel.

Figure 3.2-6 is a photograph of a 20 mm x 45 mm section taken from the same graphite epoxy panel to allow CT scanning on high resolution CT systems. Figure 3.2-7 is a high resolution CT image of the damaged composite sample taken at three locations across the laminate on CT System W; at the center of impact, 5 mm away from the center and 10 mm away from the center. The image reveals the length of the delaminations on each layer of the laminate. Several artifacts due to the specific scanning technique are also present.

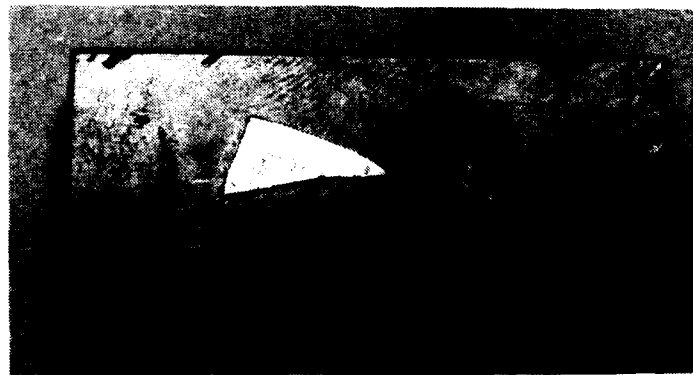
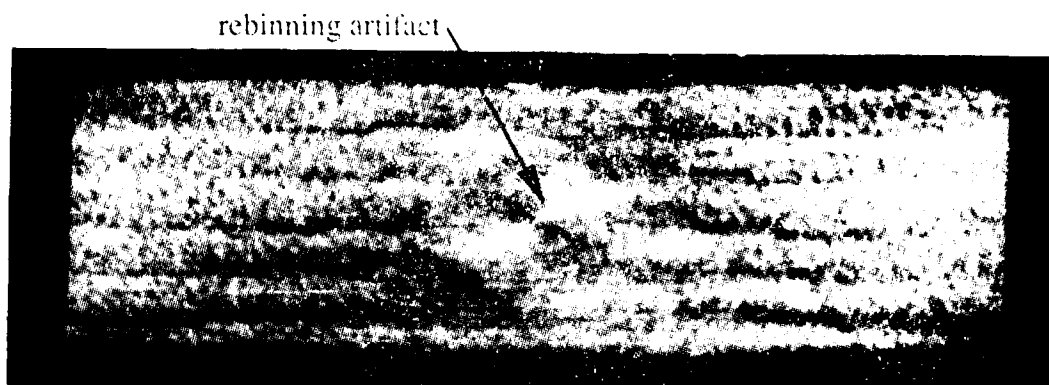
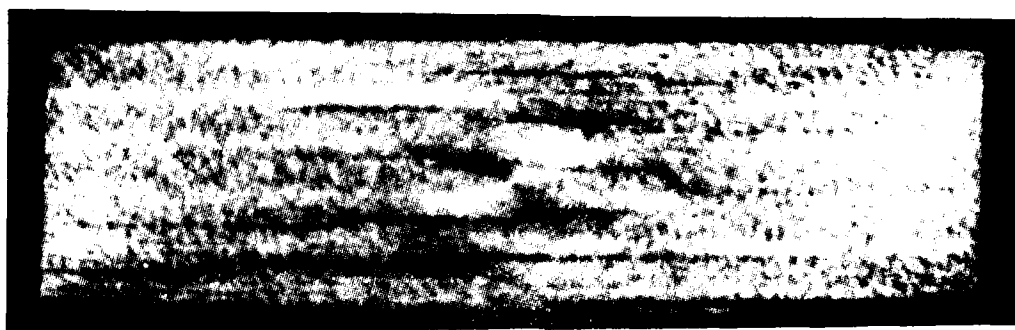


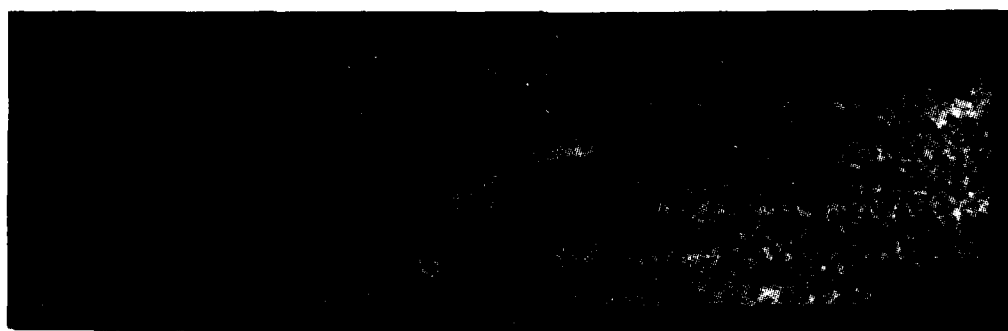
Figure 3.2-6 Photograph of a 20 mm x 45 mm section removed from the impacted panel.



a)



b)



c)

Figure 3.2-7 High resolution CT images of the impacted graphite epoxy composite sample. Top edge is the impacted surface. Image locations are: a) center, b) 5 mm off center and c) 10 mm off center.

Figure 3.2-8 , 3.2-9 and 3.2-10 are CT slices of the specimen near the center taken on CT system types V, W and X of Table 2.2-1 respectively. Reproduction of the images limits observation of the details. The images show that the systems are sensitive to the delaminations in the sample, although there are differences in the noise level and artifacts present for the 3 different systems. Approximate scan times for the three images were 65 minutes for System V, 1 minute for System W and 5 minutes for System X.

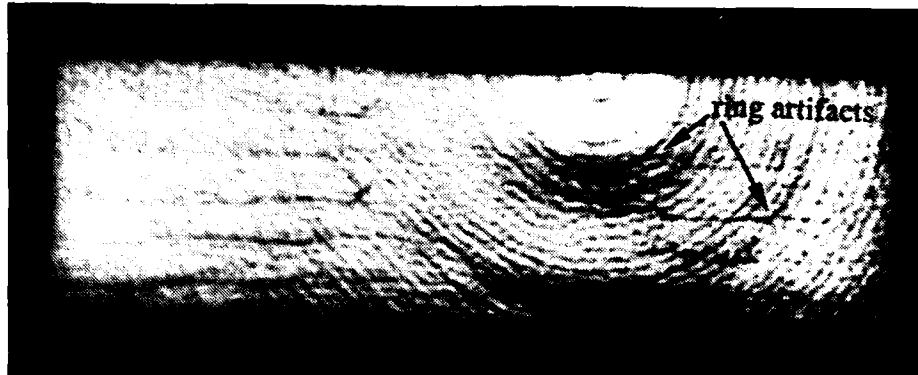


Figure 3.2-8 CT image of impact coupon for System V, 65 minute scan.

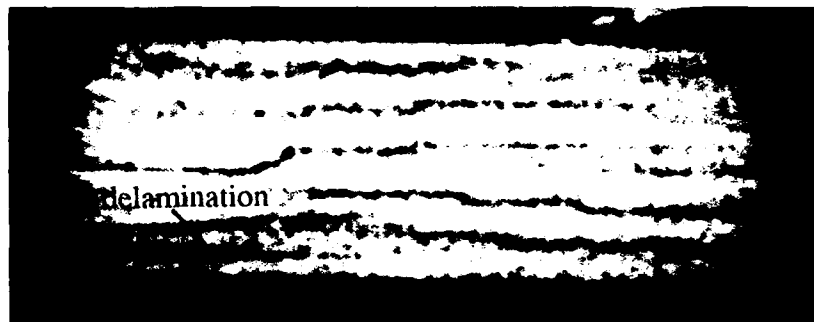


Figure 3.2-9 CT image of impact coupon from System V, 1 minute scan.

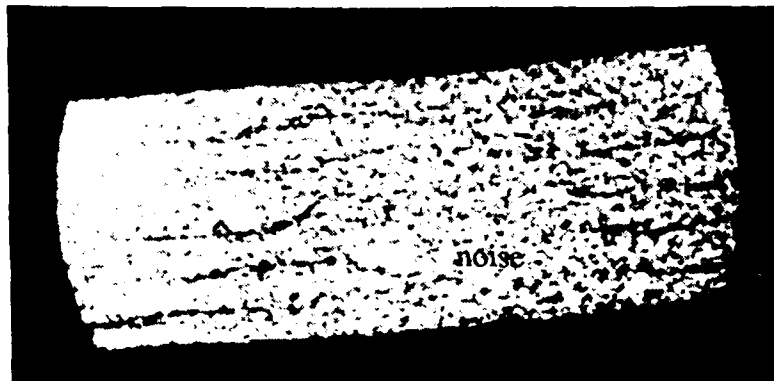


Figure 3.2-10 CT image of impact coupon from System X, 5 minute scan.

By taking a series of CT slices, it is possible to combine them to form a total three dimensional (3D) image of the component. A series of fifty CT slices were taken every 0.1 mm from the center of impact to 5 mm away from the center. This data set is a volumetric evaluation of only one-half of the total impacted region. The CT data were processed to form binary image representations of the delamination indications using mathematical morphology [27]. Mathematical morphology processes images based on feature shape. This image processing approach was chosen for delaminations because they possess a characteristic planar shape within a relatively well known orientation. The processing uses a series of steps to isolate the planar features from the noise in the image, providing a clear understanding of the location and extent of the delaminations.

The processed images were assembled into a 3D format and Figure 3.2-11 is a rendering of the delaminations viewed along the axis. If this 3D data set is rotated the delaminations in the projected view overlap and it is difficult to observe the details of the damage.

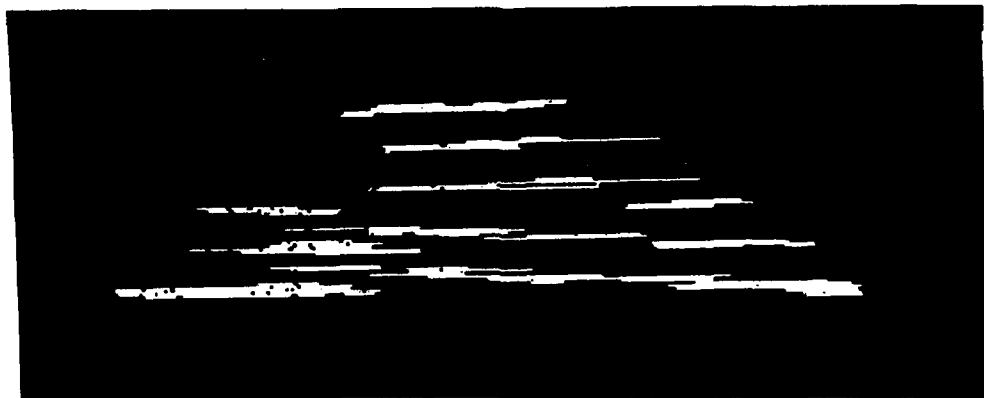


Figure 3.2-11 3D rendering of the impacted panel delaminations viewed at 0°.

The Figure 3.2-11 data was therefore analyzed to create a histogram of the pixels in the 3D image as function of depth from the impacted surface of the part. Figure 3.2-12 shows the histogram. Each peak in the histogram represents the location of a delamination plane.

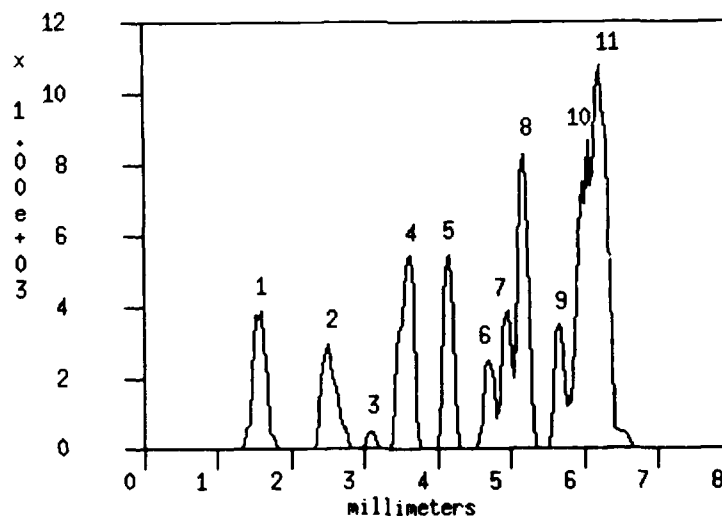


Figure 3.2-12 Histogram of the delamination indications as a function of depth.

Using the histogram information, the delamination indications can be separated according to depth in the 3D data set. Figure 3.2-12 indicates that there are 11 planes that contain significant data representative of delamination. The indications in each of the 11 planes can be consolidated to create 11 planar images. Figure 3.2-13 shows the 11 images of the delaminations.

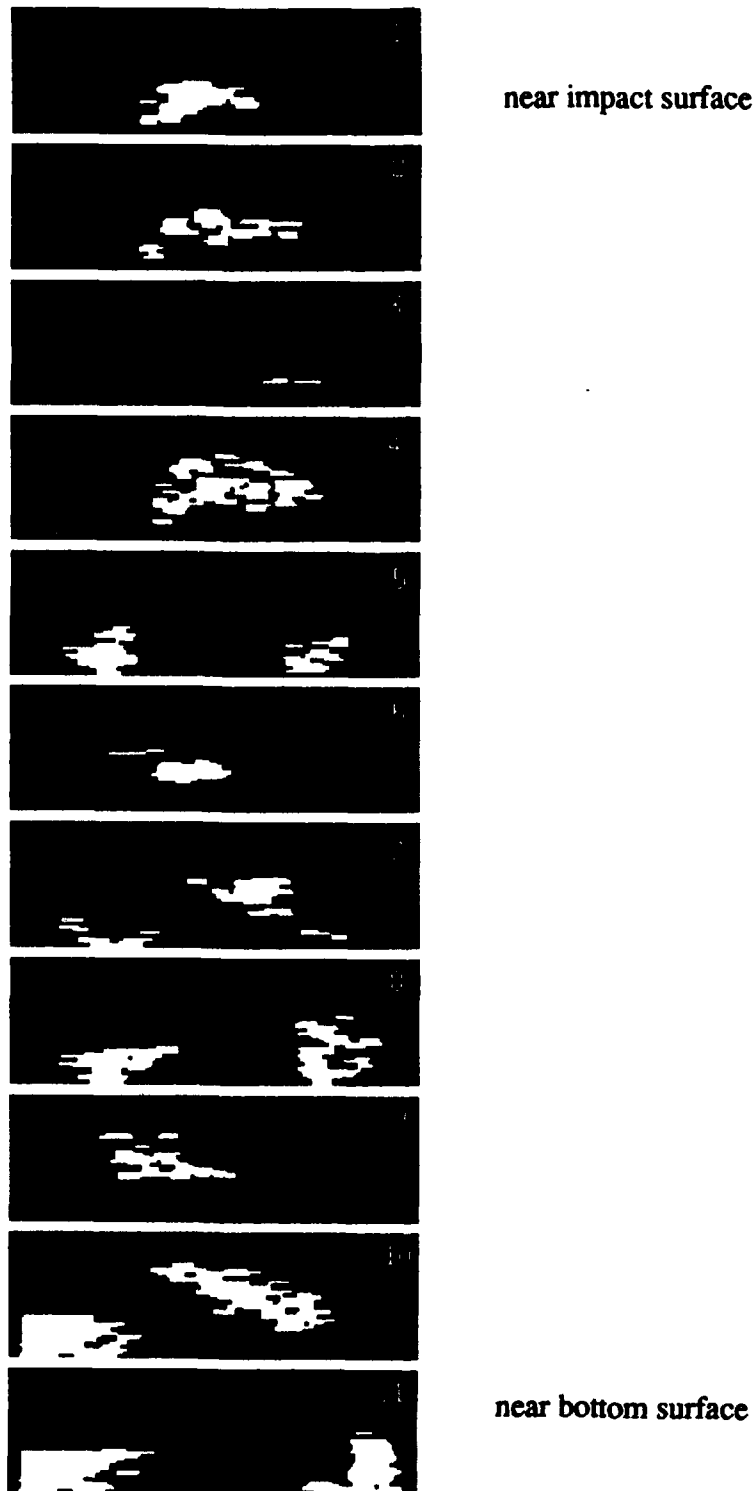


Figure 3.2-13 Eleven images of the delamination planes from the impacted panel.

The delamination planes in the Figure 3.2-13 image sequence appear to show a spiral effect, typical of laminate impact damage [28]. To assist in the visualization of the pattern, each plane of data can be given some physical thickness so that the defects will stand out in a 3D representation. This defect presentation is shown in Figure 3.2-14. The presentation indicates the amount of damage on each layer from the impacted surface. Because this data set is only 50 scans covering 5 mm from the center of impact, the images represent only a portion (approximately one-half) of the impact damaged region. The Figure 3.2-14 image is an interesting presentation of the interior of the composite sample delaminations and represents how CT might be applied to the evaluation of impact damage.



Figure 3.2-14 3D rendering of the impacted panel delaminations viewed at 15°.

This data can be used by engineers to evaluate mechanism of damage in the composite. By performing a series of damage tests on samples of various manufacturing variables, such as ply orientation, number, size and materials, the CT data can aid the development of mathematical models for the damage pattern and ultimately the development of more damage tolerant composite laminate designs.

4.0 COST BENEFIT ANALYSIS

Several of the studies undertaken in this task assignment showed high resolution CT imaging to be cost effective for obtaining needed engineering information. There are several methods for obtaining high resolution CT images as discussed in Section 2.2. The selection of the appropriate CT approach depends on the specifics of the problem. Presently, the most cost effective tool for small samples that require resolutions of 10 to 20 lp/mm appears to be a microfocus, real-time imaging based system. This system offers rapid, multiple CT images of a sample, for a modest capital investment (about a 50% cost add-on to a microfocus real-time X-ray imaging system). The following analysis assumes the use of this system.

4.1 Noninvasive Micrography

High resolution CT provides a benefit to micrographic studies in several ways. Figure 4.1-1 depicts these benefits. Because CT is nondestructive, there is the opportunity to gain not only from easier slicing, but slices can be taken without destroying the component. The additional information available from these evaluations reduces the risk any program faces. Rapid information gain can be used to accelerate schedules because decisions are made earlier, and with greater confidence. The saving of a few weeks time in the efforts of a sizable research and development staff translates into significant dollar savings. These benefits are difficult to quantify economically but are real.

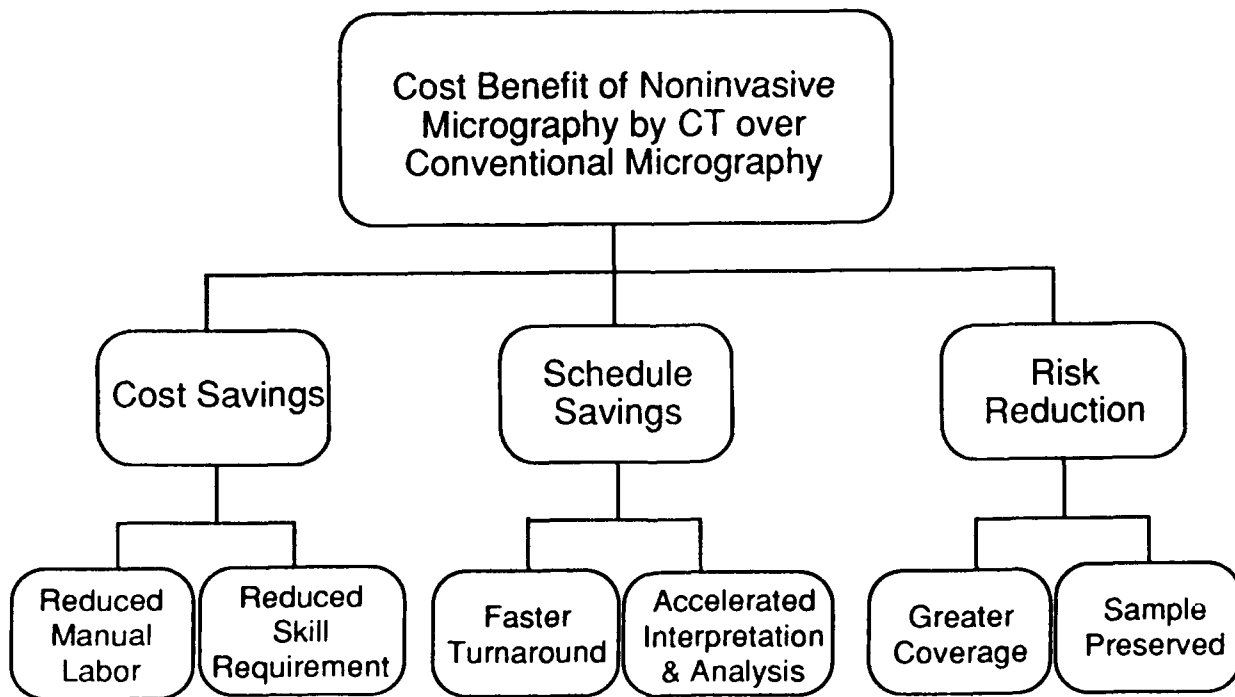


Figure 4.1-1 Cost benefits of CT for non-invasive micrography.

CT scanning can be much faster than conventional micrography and therefore offers some economic advantage. There may also be a cost savings in the skill level of the personnel used for CT relative to conventional micrography for many classes of components such as those made from advanced composite materials. For micrography of traditional engineering materials this would not be true, however for advanced composite materials CT can potentially eliminate the costs of training and maintaining specialized, skilled personnel for performing micrography. These individuals may be productive at only a 10 to 20 percent level due to the sporadic nature of qualification and failure investigations required for testing. In addition the skill level required to operate a high resolution CT system is approximately 20 to 40 percent lower than for conventional micrography of advanced composites. Absolute cost benefit comparisons may be misleading because CT images and photomicrographs are not identical. CT images must contain the information of interest desired in the micrographic study of the component. Conversely, CT images may provide unique information not available by conventional micrography.

Micrography of samples can be a costly effort for major qualification programs. Figures 4.1-2 and 4.1-3 show how CT can save time in the evaluation of samples. In Figure 4.1-2 one sample is being examined at multiple planes. The micrographic examination requires multiple polishing and photographic efforts. The CT effort only requires additional CT slices once the part has been placed on the system. For a rapid CT scanner, less than 1 minute per slice, the time per slice becomes insignificant. For multiple samples, shown in Figure 4.1-3, the time difference between micrographs and CT is not as significant, but CT can save considerable effort if a large number of samples require evaluation.

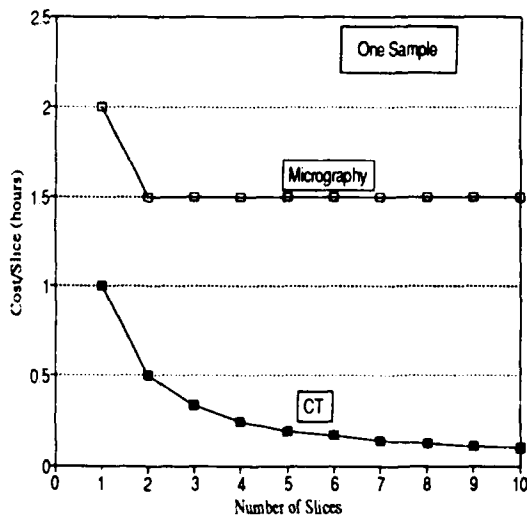


Figure 4.1-2 Comparison of the cost in hours of micrography and CT for the examination of one sample with multiple slices.

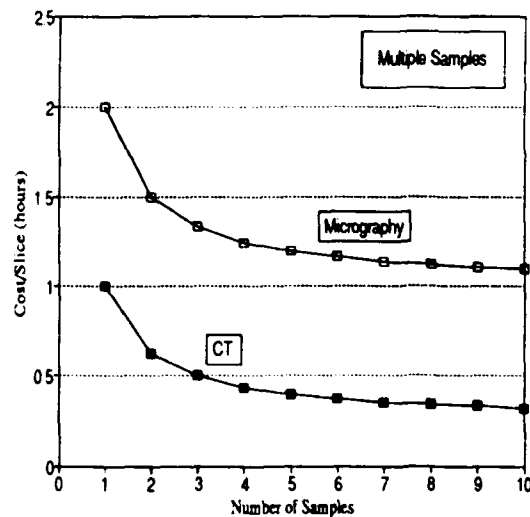


Figure 4.1-3 Comparison of the cost in hours of micrography and CT for the examination of multiple samples.

Figure 4.1-4 shows an economic comparison of having a high resolution CT capability and photomicrographic capability assuming operator cost of \$50/hour and facility costs of \$60K/year for CT and \$20K/year for photomicrography. The cross over between CT and micrography occurs at about 650 slices. Of course, it is not realistic to suggest that CT replace micrography entirely. But the economics do suggest that CT is worthwhile and not significantly more expensive than conventional approaches for obtaining information on the internal, micro-structure condition of a component or material.

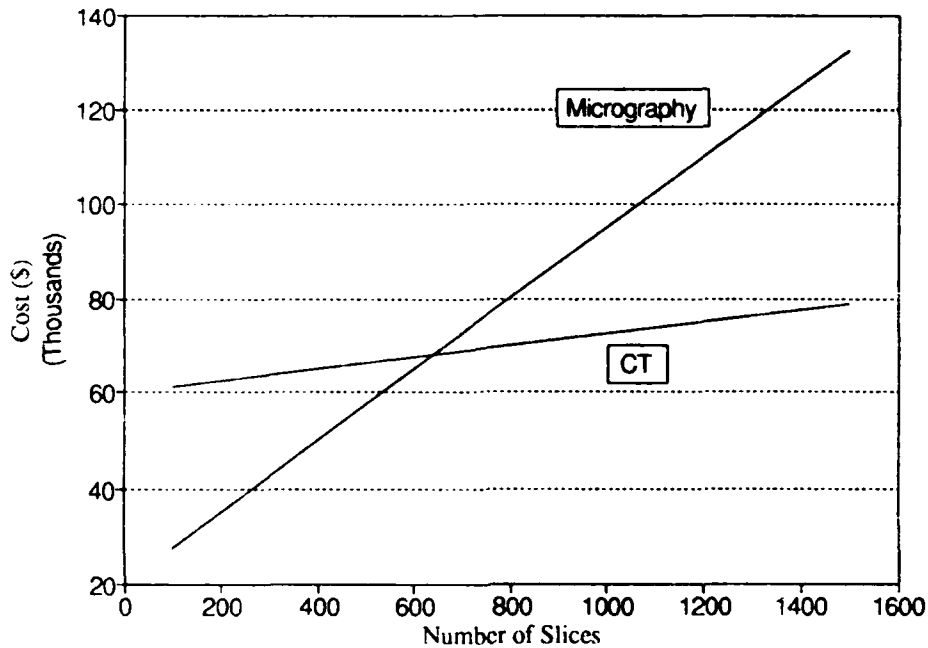


Figure 4.1-4 Comparison of the cost of slicing samples using CT or micrography as a function of the number of samples.

4.2 Failure Analysis

High resolution CT also has cost effective benefits in failure analysis. CT saves time over disassembly or sectioning. More important is that it leads to correct conclusions; the value of which may be incalculable. With CT, the component remains essentially intact, with no information destroyed by the process.

Failure analysis can sometimes require many micrographic slices to find the correct location. Under these conditions the CT approach offers considerable potential for cost savings.

Failure analysis laboratories often possess microfocus real-time radiographic capability to assist in the analysis. High resolution CT can be installed as an add-on to many systems. This allows both qualitative radiographic studies and quantitative CT capability to be available for failure analysis. The cost of adding CT to an existing real-time radiographic capability can be as little as \$150K.

5.0 CONCLUSIONS AND RECOMMENDATIONS

5.1 Conclusions

High resolution CT provides cross sectional image information useful for the evaluation of small components that rivals, and in some applications, surpasses conventional micrography. The data is obtained nondestructively and therefore can be used on parts that may have residual stresses without altering the internal configuration as would occur for destructive sectioning. The micrographic evaluations by CT are applicable to materials whose characteristics are determined by variations in X-ray linear attenuation coefficients. Composite materials are particularly suited for noninvasive micrography because CT differentiates between fibers, resins, voids and coating materials by their compositional properties rather than their optical properties. Materials that are difficult to destructively section, because the cutting and polishing process distorts the surface characteristics, are well suited to high resolution CT examination. Although metallic grain structures can not be evaluated by present high resolution CT capability, metallic interfaces such as gaps and cracks can be examined in detail. The ability to use 3D CT data sets allows micrographic information to be obtained from all orientations in a sample, which cannot be obtained by other means.

The major economic incentive to use CT is difficult to quantify directly from manufacturing cost analysis because it is primarily an engineering benefit. The nondestructive data for the material or component provides information that improves decision making and reduces overall risk. The ease and rapid acquisition of information about test samples from CT provides a means for faster, improved decisions which can accelerate a development program schedule significantly, with indirect economic benefit. For advanced materials programs that have large micrographic requirements (over 600 samples) high resolution CT can have a direct cost benefit. High resolution CT can be an effective alternative to destructive sectioning and polishing based on the relative costs of CT and destructive micrography. The actual cost benefits will depend on the specifics of the materials and the requirements of the desired analysis.

5.2 Recommendations

Organizations involved in micrographic analysis, particularly of composite materials, should consider the acquisition or contracting of services for high resolution CT. Failure analysis laboratories that require micrographic analysis of components likewise would benefit from CT analysis. CT can be used in conjunction with real-time radiography in many failure analysis investigations.

The CTAD program will continue to study high resolution CT systems under the final testing and demonstration tasks for failure analysis and material characterization. The information gained from this task assignment provides the foundation for those planned tasks.

6.0 REFERENCES

1. R. H. Bossi, R. J. Kruse and B. W. Knutson, "Computed Tomography of Electronics," WRDC-TR-89-4112, December 1989.
2. R. H. Bossi, J. L. Cline and B. W. Knutson, "Computed Tomography of Thermal Batteries and Other Closed Systems," WRDC-TR-89-4113, December 1989.
3. R. H. Bossi, J. L. Cline, E. G. Costello and B. W. Knutson, "X-Ray Computed Tomography of Castings," WRDC-TR-89-4138, March 1990.
4. R. H. Bossi, K. K. Coopridge, and G. E. Georgeson, "X-Ray Computed Tomography of Composites," WRDC-TR-90-4014, July 1990.
5. P. Burstein and R. H. Bossi, "A Guide to Computed Tomography System Specifications," WRDC-TR-90-4026, August 1990.
6. R. H. Bossi and R. J. Kruse, "X-ray Tomographic Inspection of Printed Wiring Assemblies and Electrical Components," WRDC-TR-90-4091, October 1990.
7. R. H. Bossi and G. E. Georgeson, "CT of Full-Scale Castings," WL-TR-91-4049, October, 1991.
8. Richard H. Bossi and Gary E. Georgeson, "Computed Tomography Analysis of Castings," WL-TR-91-4121, January, 1992.
9. Alan R. Crews and Richard H. Bossi, "Computed Tomography for Whole System Inspection," WL-TR-91-4109, May 1992.
10. Gary E. Georgeson and Richard H. Bossi, "Computed Tomography for Advanced Materials and Processes," WL-TR-91-4101, June 1992.
11. B. E. Foster and F. Hopkins, "High Resolution Imaging of Ceramic and Other Materials with Computed Tomography," *Proceedings of the 1991 Industrial Computed Tomography II Topical Conference*, American Society for Nondestructive Testing, May 20-24, 1991, San Diego, CA.
12. R. N. Yancey, S. J. Klima, W. H. Pfeifer and J. J. Lannutti, "Applications of High-Resolution Computed Tomography," *Proceedings of the 1991 Industrial Computed Tomography II Topical Conference*, American Society for Nondestructive Testing, May 20-24, 1991, San Diego, CA.
13. B. London, R. N. Yancey and J. A. Smith, "High-Resolution X-ray Computed Tomography of Composite Materials," *Materials Evaluation*, May, 1990.
14. L. A. Feldkamp, G. Jesion and D. J. Kubinske, "Microtomography Using A Real-Time Imaging System," *Industrial Computerized Tomography*, American Society for Nondestructive Testing Topical Proceedings, July 25-27-1989.
15. W. A. Ellingson, P. E. Engel, T. I. Hentea, K. Gopalan, P. S. Wong, S. L. Dieckman and N. Gopalsami, "Characterization of Ceramics by NMR and X-ray CT," *Industrial Computerized Tomography*, American Society for Nondestructive Testing Topical Proceedings, July 25-27-1989.

16. S. Hughes, G. Hoefft, K. Okuma and C. Smith, "Microfocus Imaging Using the ACTIS-KCT CT System," *Proceedings of the 1991 Industrial Computed Tomography II Topical Conference*, American Society for Nondestructive Testing, May 20-24, 1991, San Diego, CA.
17. J. Celeste, J. C. Kinney, G. J. Devine, C. M. Logan, R. A. Saroyan and M. C. Nichols, "X-Ray Tomographic Microscopy (XTM)," *Proceedings of the 1991 Industrial Computed Tomography II Topical Conference*, American Society for Nondestructive Testing, May 20-24, 1991, San Diego, CA.
18. B. P. Flannery, H. W. Deckman, W. G. Roberge and K. L. D'Amico, "Three-Dimensional X-ray Microtomography," *Science*, Vol. 237, September 1987, pp 1439-1444.
19. J. H. Kinney, M. C. Nichols, S. R. Stock, T. L. Starr and C. Lundgren, "The Application of X-ray Tomographic Microscopy to Chemical Vapor Infiltration Processing of Ceramic Matrix Composites," *Proceedings of the 1991 Industrial Computed Tomography II Topical Conference*, American Society for Nondestructive Testing, May 20-24, 1991, San Diego, CA.
20. J. H. Dunsmuir, S. R. Ferguson, K. L. D'Amico and J. P. Stokes, "X-Ray Microtomography: A New Tool for the Characterization of Porous Media," SPE 22860, Society of Petroleum Engineers, 66th Annual Technical Conference, October 1991.
21. K. W. Jones, B. M. Gordon, P. Spanne, M. L. Rivers and S. R. Sutton, "High-Energy Synchrotron Radiation X-Ray Microscopy: Present Status and Future Prospects," BNL-46409, presented at Workshop on Applications of Synchrotron Radiation to Chemical Engineering Science, Argonne National Laboratory, Argonne, IL, April 1991.
22. Hironao Yamji, Yasuaki Nagata, Kazuo Hayashi, Katsuhiko Kaswashima, "High Energy High Resolution Monochromatic X-Ray Computed Tomography Using Synchrotron Radiation," *Proceedings of the 1991 Industrial Computed Tomography II Topical Conference*, American Society for Nondestructive Testing, May 20-24, 1991, San Diego, CA.
23. G. Fuhrmann, H. Halling and R. Moeller, "X-Ray Microtomography with SEM for Laboratory Material Research," *Proceedings of the 1991 Industrial Computed Tomography II Topical Conference*, American Society for Nondestructive Testing, May 20-24, 1991, San Diego, CA.
24. A. Y. Sane, D. J. Eichenmiller and A. W. Gee, "Carborundum Ceramic Filter: Part I - Structure and Properties," *Light Metals 1991*, ed. E. L. Rooy, The Minerals, Metals and Materials Society, NY, pp. 1139-1150, 1990.
25. P. Engler, M. W. Santana, D. J. Eichenmiller and A. Y. Sane, "Quantification and Visualization of the Structure of Porous Ceramic Filters Using Computed Tomography," *Proceedings of the 1991 Industrial Computed Tomography II Topical Conference*, American Society for Nondestructive Testing, May 20-24, 1991, San Diego, CA.
26. C. F. Buynak, T. J. Moran, and R. W. Martin, "Delamination and Crack Imaging in Graphite-Epoxy Composites," *Materials Evaluation*, April, 1989.

27. R. M. Haralick, S. R. Sternberg and X. Zhuang, "Image Analysis Using Mathematical Morphology," IEEE Transactions on Pattern Analysis, and Machine Intelligence, Vol. PamI-9, No. 4, July 1987.
28. E. F. Dost, L. B. Iclewicz and J. H. Gosse, "Sublamine Stability Based Modeling of Impact-Damaged Graphite Laminates," Proceedings of the American Society for Composites 3rd Technical Conference, Seattle, WA, 1988.

APPENDIX A

Component Test List for High Resolution CT Scanning

PID #	Part Name	Scan Objective	Material	Size (mm)
Electronics/Optics				
010203	Small Relay	Contact position/clearance	Steel/silver	10
010304c	Transformer	Cracked core		
010305	Miniature Torroidal Coil	Ferrite microcracking	Copper/steel	20 x 15
010401	Ceramic Transistor	Cracking	BeO	5 x 3
010405	Capacitive Filter			10
010406	10 pF Chip Capacitor	Voids, microcracks	Barium nitrate	2 x 1.5 x .5
010407	1000 pF Chip Capacitor	Voids, microcracks	Barium nitrate	2 x 1.5 x .5
010407	0.01 pF Chip Capacitor	Voids, microcracks	Barium nitrate	2 x 1.5 x .5
010802	Fiber Optic Connector	Epoxy voiding, bond quality	SiO ₂	2 dia.
Advanced Materials				
040127	Impacted Panel	Impact damage	Graphite/epoxy	30 x 60
050102a-d	TiMMC	Fiber consolidation	SiC/Ti-6Al-4V	33 x 55 x 1
050103	Diff. Bond MMC (1500°)	Fiber consolidation and bond	Ti/SiC MMC	95 x 25 x 7
050104	Diff. Bond MMC (1700°)	Fiber consolidation and bond	Ti/SiC MMC	50 x 40 x 7
050105a&b	Ti MMC Panel	Fiber consolidation	Ti/SiC MMC	45 x 85 x 1
050204	ATF Test Coupon	Density variation	Graphite/epoxy	23 x 73 x 7
050205	Ceramic Filter	Pore size and Al particulates	Ceramic	25 x 8 x 6
050314a&b	Comp. Test Samples	Fiber orientation	C	7 x 5 x 35
050315a	Comp. Tensile Specimen	Coating thick., quality	SiC,C	7 x 3 x 30
050315b	Comp. Tensile Specimen	Coating thick., quality	SiC,C	7 x 7 x 30
050316	Coating Samples	Coating thick., quality	SiN,C	45 x 22 x 2
050317	Coating Samples	Coating thick., quality	SiN,C	45 x 22 x 2
050318	Coated Composite J	Coating thickness & quality	C composite	100 x 65 x 10
050319	Coated Composite C	Coating thickness & quality	C composite	125 x 25 x 75
Miscellaneous				
030124	Coupon with defect	Crack (0.025 mm)	Al	30 x 20 x 12
060307	Lug Plate	Crack (0.025 mm)	Al	74 x 74 x 12
060309	Rivet	Gaps	Al	37
Standards				
000010	Cylinder	Line pair/MTF	Al	9.5 dia.
	Cylinder	Line pair/MTF	Al	4 dia.
000102	Line Pair Gauge	Resolution	Al/Acrylic	30 x 30 x 30
000103	Crack Direction Standard	Cracks (0.025 mm)	Al	17 x 26 x 18
000601	Cylinder	Noise/MTF	Al	12 dia.
000803	Pins & Holes	Artifacts	Al/Acrylic	25 dia.

APPENDIX B

Summary of High Resolution CT (HRCT) Examples

ITEM	PROBLEM	OBJECTIVE	APPROACH	PAYOFF		
				Sched.	Cost	Risk Reduct.
Advanced Composites:	High risk of airplane structure failure because of inadequate inspection	Increase defect detection capability			x	
	High cost of micrography for material qualification	Reduce overall program material qualification costs	Utilize HRCT scanning services	x	x	
	High cost of micrography for cost failure mode identification	Reduce micrography by half	Use HRCT to replace 3/4 of samples	x	x	
	Risk of composite oxidation protective coating failure	Reduce coating variability	Justify HRCT costs for installation at manufacturers			
	Materials allowables testing currently inadequately identifies failure modes leading to unacceptable margins of safety or high risk of unanticipated failure	Use CT to provide greater confidence in failure mode understanding	Use HRCT in conjunction with materials allowables studies			x
Metal Fasteners:	Inability to measure compressed fastener fit and residual stress leading to risk of failure	Increase precision of estimate of residual stress and incorporate into process control	Perform HRCT test on samples in the stressed condition to monitor internal gaps			x
Component Failure Analysis:	Cost of mechanical sectioning, risk of mislocating features and schedule loss	Reduce the risk of missing critical features or characteristics and reduce micrographic schedule and costs	Use HRCT services	x	x	x